ACS OMEGA

Open Access

http://pubs.acs.org/journal/acsodf

Article

Multifunctional Crystalline Coordination Polymers Constructed from 4,4′-Bipyridine-*N*,*N*′-dioxide: Photochromism, White-Light Emission, and Photomagnetism

Ning-Ning Zhang,* Liu-Di Xin, Li Li, Ya-Nan Zhang, Ping-Ping Wu, Yong-Fang Han, Yong Yan,* and Kong-Gang Qu

Cite This: *ACS Omega* 2023, 8, 34017−34021

Read Online

ACCESS | Metrics & More | Article Recommendations | Supporting Information

ABSTRACT: Multifunctional photochromic coordination polymers (CPs) have shown great potential in many areas, like molecular switches, anticounterfeiting, magnetics, and optoelectronics. Although multifunctional photochromic CPs can be obtained by introducing photoresponsive functional units or by exploiting the synergy effect of each component, relatively limited photochromic ligands hinder the development of various multifunctional photochromic CPs. In this work, we reported two multifunctional coordination polymers $\{[Zn(bpdo)(fum)(H_2O)_2]\}_n$ (**1**) and $\{[Mn(bpdo)(fum)(H_2O)_2]\}_n$ (**2**) based on an easily accessible but underestimated photoactive molecule 4,4′-bipyridine-*N*,*N*′-dioxide (**bpdo**). Compound **1** exhibits photochromism and white-light emission with an ultra-high color rendering index (CRI) of 92.1. Interestingly, compound **1** could emit intrinsic white light in the crystalline state upon UV irradiation both before and after photochromism. Meanwhile, compound **2** displays photochromic and photomagnetic properties, induced by the photogenerated radicals via a photoinduced electron transfer mechanism.

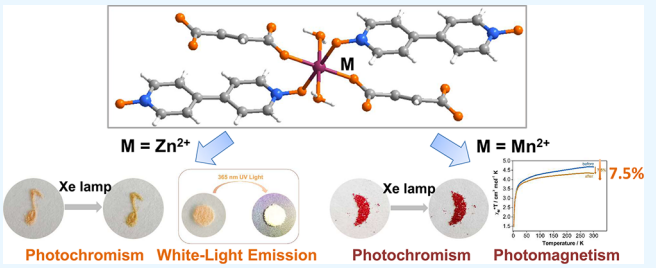

1. INTRODUCTION

Multifunctional photochromic compounds, as an important branch of photoresponsive materials, have attracted extensive attention due to their potential applications in the fields of molecular switches, anticounterfeiting, and magnetism.[1−5] Compared with pure inorganic or organic photochromic compounds, photochromic coordination polymers (CPs) can not only maintain or improve the characteristics of each component but also generate new photoresponsive properties such as tunable white-light emission or photomagnetism features, due to the synergistic effect of each component.[6−10] It has been shown that multifunctional CPs can be effectively synthesized by introducing functional ligands.[11,12] However, in addition to traditional viologen, diarylethene, and azobenzene derivatives, the available functional photochromic ligands are relatively limited, thus preventing further exploration of multifunctional photochromic CPs. It is still desirable to explore a variety of multifunctional photochromic CPs with new functional photochromic organic ligands.

Owing to the synthesis of multifunctional photochromic CPs usually requires the presence of suitable coordinating groups in the ligands, various coordinating groups such as pyridine, carboxylic acid, and imidazole have to be attached to photochromic molecules through a series of complex organic reactions.[13] Recently, we discovered an easily accessible photoactive molecule 4,4′-bipyridine-*N*,*N*′-dioxide (**bpdo**) that can be obtained by simple oxidization of 4,4′-bipyridine.[14] The **bpdo** exhibits an obvious photochromic phenomenon with stable charge-separated state.[15] On the other hand, according to the literature,[16] **bpdo** exhibits diverse coordination types with metal ions via the O atoms of *N*-oxide groups, making it suitable for constructing of multifunctional photochromic CPs. To date, although approximately 400 **bpdo**-based complexes have been deposited in the CCDC database, their photochromic and derived versatility has been underexplored.[17] In this work, two new two-dimensional (2D) isostructural crystalline CPs $\{[Zn(bpdo)(fum)(H_2O)_2]\}_n$ (**1**) and $\{[Mn(bpdo)(fum)(H_2O)_2]\}_n$ (**2**) (fum: fumaric acid) based on **bpdo** and fum ligands with different metal ions (Zn^{2+}, Mn^{2+}) have been synthesized. They both have evident photochromic properties. Compound **1** displays white-light emission with an ultra-high color rendering index (CRI) of 92.1. Interestingly, complex **1** can emit intrinsic white light in the crystalline state upon UV irradiation both before and after photochromism. Due to the synergy between

Received: July 7, 2023
Accepted: August 29, 2023
Published: September 7, 2023

https://doi.org/10.1021/acsomega.3c04892
ACS Omega 2023, 8, 34017−34021

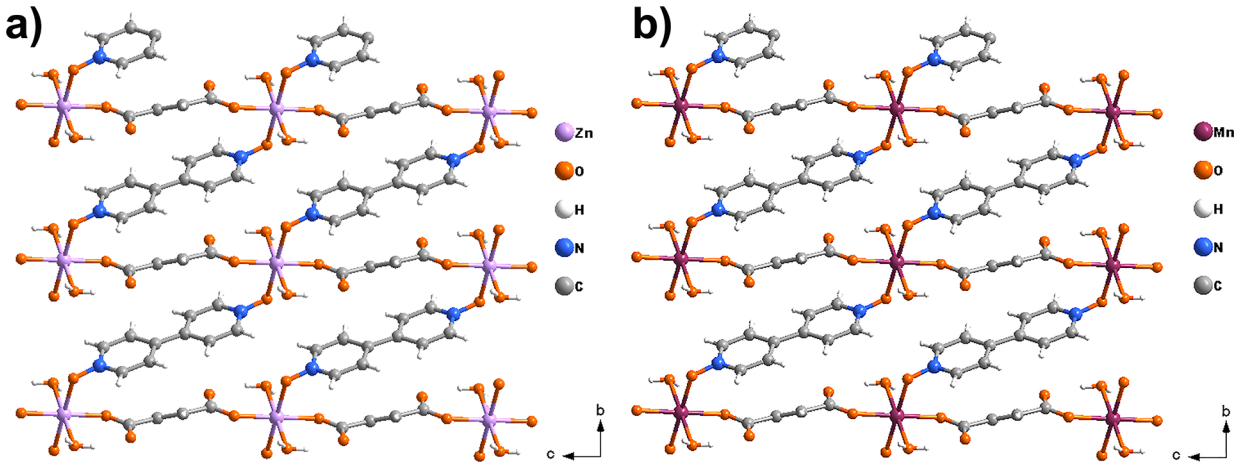

Figure 1. Perspective view of the 2D-layered structure in compounds **1** (a) and **2** (b) developing in the [100] plane.

the photochromic ligand and the Mn(II) ion, compound **2** also exhibits photomagnetism.

2. RESULTS AND DISCUSSION

2.1. Crystal Structures of 1 and 2. From the results of single-crystal X-ray diffraction (SXRD), compounds **1** and **2** are isostructural and both crystallize in the triclinic crystal system, space group $P\bar{1}$ (Table S1). Each Zn^{2+} or Mn^{2+} is 6-fold coordinated and connects two O atoms from two **bpdo**, two O atoms from two fumaric acid carboxyl groups, and two O atoms from two coordinating water molecules. They both present 2D-layered structures (Figure 1) parallel to crystallographic planes [100], composed of **bpdo** ligands and fumarate dianions that behave as bis-monodentate spacers connecting $Zn(H_2O)_2$ (Figure 1a) and $Mn(H_2O)_2$ (Figure 1b) units, respectively, the metals being located on a center of symmetry. The synthesis methods of compounds **1** and **2** are provided in the Supporting Information (for the details, see SI). The phase purity of compounds **1** and **2** was confirmed by powder X-ray diffraction (PXRD), infrared (IR) spectra, and thermogravimetric (TG) (Figures S1−S6, for the details, see Supporting Information). Therefore, their crystalline samples were directly used for tests on photochromic, white-light emission, and photomagnetic properties.

2.2. Photochromic Properties of 1 and 2. Before irradiation, the fresh crystalline sample of **1** was pink. After irradiation by the 210 W (15 V × 14 A) Xe lamp for 1 and 5 min under ambient conditions, the color gradually turned into yellowish green (Figure 2a). At the same time, the bands of the electronic absorption spectra of **1** between 400 and 1200 nm had a gradual enhancement under irradiation (Figure 2b). In order to rule out the cause of structural change, we performed PXRD and IR tests before and after irradiation. As shown in Figures S1 and S2, there are no new peaks created and old peaks disappeared, which precludes the possibility of photoisomerization or photolysis. Furthermore, we tested EPR to explain the color change and the increase in absorption bands. Before irradiation, compound **1** had no radical signal. By contrast, the irradiated sample **1** had a strong radical signal at g = 2.0037 (Figure 2c). Therefore, the change in color and the increase in absorption bands of **1** could be attributed to the formation of radicals generated by photoinduced electron transfer. In addition, colored **1** can partially fade. It is difficult to fade to the original state after placing in the dark for almost 2 months at

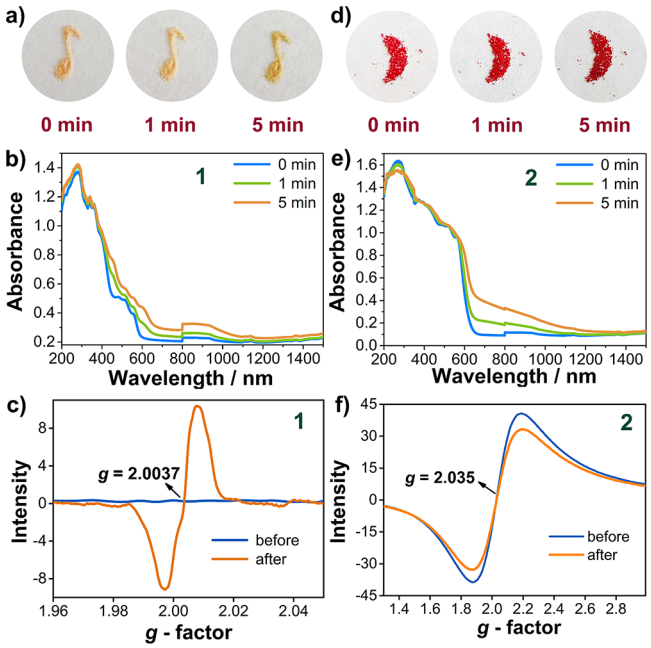

Figure 2. Colors (a and d), electronic absorption spectra (b and e), and EPR spectra (c and f) of **1** and **2** before and after irradiation in the crystalline state, respectively.

room temperature in air (Figure S7a) or after heat at 120 °C for 7 h (Figure S7b), which implies the presence of an ultra-long-lived and stable charge-separated state.[18]

As for **2**, the coordinate metal ion is Mn(II). After irradiation by the 210 W (15 V × 14 A) Xe lamp under ambient conditions, the brightly red crystalline-state sample of **2** gradually turned into dark red (Figure 2d). The PXRD (Figure S4) and IR (Figure S5) experiments have shown that no significant crystal structure change occurs in the irradiated sample, and thus, the possibility of photolysis or photoisomerization can be excluded. Similar to **1**, the band of the electronic absorption spectra of **2** between 550 and 1200 nm had a gradual enhancement under irradiation (Figure 2e). Therefore, the color change may be caused by photoinduced electron transfer. To confirm this further, solid-state X-band EPR continuous spectrum tests for compound **2** were performed at room temperature. As shown in Figure 2f, there is already a broad resonant absorption band signal at g = 2.035 existing before irradiation, which is attributed

https://doi.org/10.1021/acsomega.3c04892
ACS Omega 2023, 8, 34017−34021

to the Mn^{2+} ions in the octahedral coordination geometry.[19] After continuous light irradiation for 5 min at room temperature, the peak intensity decreases, probably due to the antiferromagnetic couplings between Mn^{2+} ions and the photogenerated radicals. Thus, as for magnetic metal ions, a **bpdo**-based complex could also perform the behavior of electron transfer photochromism.

To investigate the mechanism of the photo-induced generated radicals of compounds **1** and **2** and the process of electron transfer in the crystalline state, density of states (DOS) was calculated at the GGA/PBE level based on the SXRD data in virtue of the CASTEP package.[20] As for **1**, the Γ_a state mainly consisted of the bonding *p* orbitals of fumaric acid and oxygen atoms of **bpdo**, the Γ_b and Γ_c states mainly consisted of the bonding *p* orbitals of fumaric acid, while the component in the Γ_d state was the antibonding p_π orbitals of bipyridyl of bpdo (Figure 3a). As for **2**, the components for the Γ_a, Γ_b, Γ_c, and Γ_d states are similar to that of **1** (Figure 3b). That is, for both **1** and **2**, the pathway of electron transfer is mainly from fumaric acid to bipyridyl of **bpdo**. The oxygen atoms of **bpdo** acted as a fraction of electron donors but mainly increased the electron-accepting ability of **bpdo**.

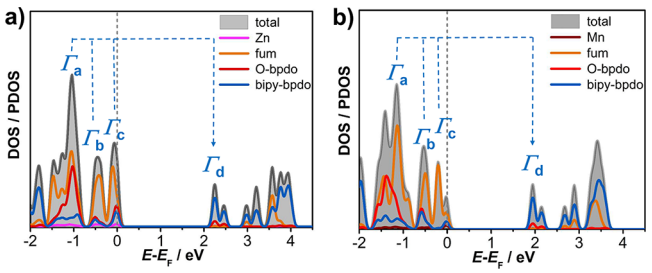

Figure 3. Total and partial DOS of **1** and **2** (a and b), respectively. The Fermi level (E_F) is set to zero by default.

2.3. White-Light Emission of $\{[Zn(bpdo)(fum)(H_2O)_2]\}_n$ (1).

The photoluminescence properties of **1** were researched in the crystalline state. As illustrated in Figure 4a, the fresh sample **1** displays broad emission spectra, covering the whole visible range from 400 to 800 nm upon irradiation with UV light (330−370 nm) at room temperature. The intensities of the emission bands peaked at 440 nm which can be tuned by the excitation varying from 330 to 370 nm. The best excitation wavelength is 330 nm (Figure S8). When the excitation wavelength is 330 nm, the peak values and full widths at half-maximum (FWHMs) are 440 and 144 nm, respectively. At this point, the Commission Internationale de l'Eclairage (CIE) coordinates and an appropriate correlated color temperature (CCT) for **1** are (0.24, 0.25) and 26,230, respectively, suggesting the emission of "cold" white light (Figure S9 and Table S2). Meanwhile, it has a high corresponding CRI of 91.3 (Table S2). It is interesting to note that sample **1** always emits white light at any excitation wavelength from 330 to 370 nm, and their CRI values fall in the range of 88−92 (Figures 4a,c, S9 and Table S2). As shown in Figure 4b, when excited by a 365 nm UV lamp, the crystalline sample **1** shows white light emission.

Under the same test conditions, especially the same slit size, we tested the photoluminescence properties of the irradiated crystalline sample of **1**. Compared with that of the fresh sample, its fluorescence emission situation has the following differences. First, the fluorescence intensity decreased overall, either one of the excitations varying from 330 to 370 nm (Figure 4c,d), which could be attributed to photoinduced electron transfer. Second, although they are still in the white light range, the CIEs have shifted up (Figure S9 and Table S2). Third, both CCTs and CRIs have declined (Table S2). It is worth emphasizing that compound **1** exhibits photochromism only when exposed to a high-power Xenon lamp. The luminescence color of compound **1** does not change under normal ultraviolet. Therefore, the white light emission of fresh sample **1** can be used like other single-component white light materials.

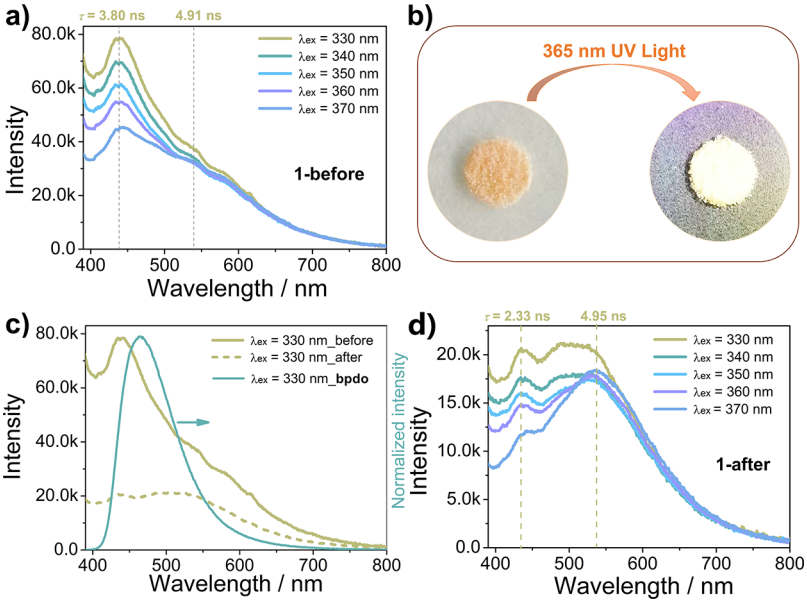

Figure 4. (a) Solid-state photoluminescence spectra of sample **1** before photochromism excited at 330−370 nm. (b) Photographs of **1** in ambient light and under 365 nm UV light. (c) Contradistinctive solid-state photoluminescence spectra excited at 330 nm of **1** before and after photochromism, and **bpdo**, respectively. (d) Solid-state photoluminescence spectra of **1** after photochromism excited at 330−370 nm.

https://doi.org/10.1021/acsomega.3c04892
ACS Omega 2023, 8, 34017−34021

To study the mechanism of the dual emission of **1**, the decay curves were recorded and the average decay lifetime was determined to be 3.80 ns at 440 nm and 4.91 ns at 540 nm before photochromism (Figures 4a, S10a,b), to be 2.33 ns at 440 nm and 4.95 ns at 540 nm for after photochromism (Figures 4d, S10c,d), respectively, implying that are all fluorescent emission, but the emission peak at 440 nm and shoulder peak at 540 nm come from two distinct origins. As shown in Figure 4c, when excited at 330 nm, the ligand **bpdo** has an emission peak at 463 nm. Thus, the emission peak at 440 nm can be assigned to ligand-centered emission. Compared with free ligand bpdo, the new shoulder peak at 540 nm in compound **1** can be ascribed to the excited state of the ligand-to-metal charge transfer (LMCT).[21]

2.4. Photomagnetic Effect of {[Mn(bpdo)(fum)-(H_2O)$_2$]}$_n$ (2). Room-temperature photochromic and photomagnetic bifunctional materials have captured widespread attention for practical applications. However, due to the difficulty in synthesis, only a few photochromic and photomagnetic bifunctional compounds have been reported.[19,22,23] We aimed to search new multifunctional systems exhibiting both photochromic and photomagnetic properties by using the reported three-in-one synthetic strategy,[19] with paramagnetic metal ions (Mn^{2+}) as spin carriers, **bpdo** ligands as photoresponsive components, and fumaric acid (**fum**) as mixed pathways for extended superexchange. Thus, a Mn(II) coordination polymer of formula [Mn(bpdo)(fum)(H_2O)$_2$]$_n$ (**2**) was synthesized to research the photomagnetic properties.

In order to investigate the photomagnetic effect of compound **2**, the magnetic studies before and after irradiation by the Xe lamp at room temperature are performed using the powdered crystalline sample. The magnetic susceptibilities of **2** were measured in the 2−300 K temperature range under 1000 Oe and are shown as $\chi_M T$ versus T plots in Figure 5. Before irradiation,

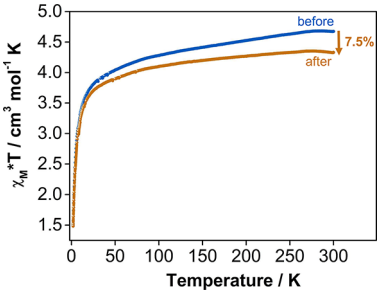

Figure 5. Plots of $\chi_M T$ versus T of compound **2** before and after irradiation.

the value of $\chi_M T$ at 300 K is 4.68 cm^3 mol^{-1}·K, close to the spin-only value (4.38 cm^3 mol^{-1} K) for one magnetically isolated high-spin Mn(II) ions (S = 5/2).[19,24] On cooling, the $\chi_M T$ value first remained essentially constant in the temperature range of 300 to 50 K, then decreased rapidly and reached 1.49 cm^3 mol^{-1} K, showing dominant antiferromagnetic behaviors of Mn(II) ion. After illumination by Xe lamp in the air for 5 min, the $\chi_M T$ value at 300 K is 4.33 cm^3 mol^{-1}·K, fell by 7.5%. According to the electronic absorption spectra, EPR spectra, and DOS, photogenerated radicals in **2** are produced from the electron-rich **fum** units and transferred to the electron-deficient **bpdo** ligands, showing a metal-assisted ligand-to-ligand electron transfer process. Thus, the falling of $\chi_M T$ at 300 K for **2** after coloration may be attributed to the stronger antiferromagnetic interaction between the photo-generated radicals and the Mn(II) ion.[19]

3. CONCLUSIONS

In summary, two new multifunctional photochromic 2D crystalline coordination polymers based on photoactive 4,4′-bipyridine-*N*,*N*′-dioxide (**bpdo**) ligands with different metal ions (Zn^{2+}, Mn^{2+}) were synthesized. Compound **1** displays photochromism and single-component white-light emission with an ultra-high CRI of 92.1. Compound **2** shows detectable photochromic behavior and exhibits obvious photomagnetism due to the stronger antiferromagnetic interaction between the photogenerated radicals and the Mn(II) ion. Given the coordination versatility of photochromic molecule **bpdo**, we believe this work provides an effective pathway way to achieve multifunctional photoactive coordination polymers by incorporating **bpdo** units.

4. EXPERIMENTAL SECTION

4.1. Materials. All chemicals were purchased commercially and used without further treatment except **bpdo**. Bpdo was prepared according to the reported method.[15]

4.2. Synthesis of {[Zn(bpdo)(fum)(H_2O)$_2$]}$_n$ (1). 4,4′-Bipyridine-*N*,*N*′-dioxide (**bpdo**, 0.1 mmol, 20 mg) and fumaric acid (fum, 0.1 mmol, 11 mg) dissolved in the mixture of 1 mL distilled water, 3 mL anhydrous ethanol, and 3 mL DMF, then got solution A. $ZnSO_4$·7H_2O (0.094 mmol, 27 mg) dissolved in 2 mL distilled water, then got solution B. And then, solution B slowly drops into solution A. Their mixture reacted at 90 °C in a 10 mL sealed glass vial for 24 h. The block pink crystals of compound **1** were obtained after filtration. The yield was 58%, based on **bpdo**. The purity of sample **1** can be identified by PXRD (Figure S1), IR data (Figure S2), and elemental analyses. Calcd (%) for **1**: C, 41.66; N, 6.94; H, 3.50; found (%): C, 41.51; N, 6.86; H, 3.42. In addition, the crystals of **1** can remain stable till about 185 °C (Figure S3).

4.3. Synthesis of {[Mn(bpdo)(fum)(H_2O)$_2$]}$_n$ (2). Compound **2** was prepared using the same synthetic procedure of **1** but from $MnCl_2$ (0.094 mmol, 12 mg). The crystals obtained are bright red blocks. The yield was 51%, based on **bpdo**. The purity of sample **2** can be identified by PXRD (Figure S4), IR data (Figure S5), and elemental analyses. Cal. (%) for **2**: C, 42.76; N, 7.12; H, 3.59; found (%): C, 42.77; N, 7.15; H, 3.49. In addition, the crystals of **2** can remain stable till about 200 °C (Figure S6).

■ ASSOCIATED CONTENT

Supporting Information

The Supporting Information is available free of charge at https://pubs.acs.org/doi/10.1021/acsomega.3c04892.

Experimental and computational methods, crystal data table, PXRD, IR, TG spectra, ESR spectra, excitation spectrum, CIE coordinates maps, lifetime curves, CIE coordinates, and CT and CRI table (PDF)

crystallographic data for compound **2** (CIF)

crystallographic data for compound **1** (CIF)

■ AUTHOR INFORMATION

Corresponding Authors

Ning-Ning Zhang − *School of Chemistry and Chemical Engineering, Liaocheng University, Liaocheng, Shandong 252059, P. R. China;* orcid.org/0000-0002-3872-7884; Email: zhangningning@lcu.edu.cn

https://doi.org/10.1021/acsomega.3c04892
ACS Omega 2023, 8, 34017−34021

Yong Yan − *School of Chemistry and Chemical Engineering, Liaocheng University, Liaocheng, Shandong 252059, P. R. China*; Email: yanyong@lcu.edu.cn

Authors

Liu-Di Xin − *School of Chemistry and Chemical Engineering, Liaocheng University, Liaocheng, Shandong 252059, P. R. China*

Li Li − *School of Materials Science and Engineering, Henan Polytechnic University, Jiaozuo 454000, P. R. China*

Ya-Nan Zhang − *School of Chemistry and Chemical Engineering, Liaocheng University, Liaocheng, Shandong 252059, P. R. China*

Ping-Ping Wu − *School of Chemistry and Chemical Engineering, Liaocheng University, Liaocheng, Shandong 252059, P. R. China*

Yong-Fang Han − *School of Chemistry and Chemical Engineering, Liaocheng University, Liaocheng, Shandong 252059, P. R. China*

Kong-Gang Qu − *School of Chemistry and Chemical Engineering, Liaocheng University, Liaocheng, Shandong 252059, P. R. China*

Complete contact information is available at: https://pubs.acs.org/10.1021/acsomega.3c04892

Funding

This work was financially supported by the Natural Science Foundation of Shandong Province (ZR2022QB041, ZR2023QB195) and the Open Foundation of State Key Laboratory of Structural Chemistry (20210009).

Notes

The authors declare no competing financial interest.

■ ACKNOWLEDGMENTS

This work was financially supported by the Natural Science Foundation of Shandong Province (ZR2022QB041 and ZR2023QB195) and the Open Foundation of State Key Laboratory of Structural Chemistry (20210009).

■ REFERENCES

(1) Zhao, J. L.; Li, M. H.; Cheng, Y. M.; Zhao, X. W.; Xu, Y.; Cao, Z. Y.; You, M. H.; Lin, M. J. Photochromic crystalline hybrid materials with switchable properties: Recent advances and potential applications. *Coord. Chem. Rev.* **2023**, *475*, No. 214918.

(2) Han, S. D.; Hu, J. X.; Wang, G. M. Recent advances in crystalline hybrid photochromic materials driven by electron transfer. *Coord. Chem. Rev.* **2022**, *452*, No. 214304.

(3) Li, L.; Yu, Y. T.; Hua, Y.; Li, X. N.; Zhang, H. Recent progress in polyoxometalate−viologen photochromic hybrids: structural design, photochromic mechanism, and applications. *Inorg. Chem. Front.* **2023**, *10*, 1965−1985.

(4) Yu, T. L.; Guo, Y. M.; Wu, G. X.; Yang, X. F.; Xue, M.; Fu, Y. L.; Wang, M. S. Recent progress of d10 iodoargentate(I)/iodocuprate(I) hybrids: Structural diversity, directed synthesis, and photochromic/thermochromic properties. *Coord. Chem. Rev.* **2019**, *397*, 91−111.

(5) Han, S. D.; Hu, J. X.; Li, J. H.; Wang, G. M. Anchoring polydentate N/O-ligands in metal phosphite/phosphate/phosphonate (MPO) for functional hybrid materials. *Coord. Chem. Rev.* **2023**, *475*, No. 214892.

(6) Pan, Q. Y.; Sun, M. E.; Zhang, C.; Li, L. K.; Liu, H. L.; Li, K. J.; Li, H. Y.; Zang, S. Q. A multi-responsive indium-viologen hybrid with ultrafast-response photochromism and electrochromism. *Chem. Commun.* **2021**, *57*, 11394−11397.

(7) Shen, J.; Kang, X.; Hao, P.; Fu, Y. Semiconductive donor promoted photochromism of iodoplumbate hybrids. *Inorg. Chem. Front.* **2020**, *7*, 4865−4871.

(8) Li; Liang, Z. G.; Liu, Y.; Li, J. H.; Pan, J.; Han, S. D. Ligand Tailoring and Functional Group Fusion Strategy for Developing Photochromic Compounds: A Case Study for Pyridinedicarboxylic Acid. *Cryst. Growth Des.* **2023**, *23*, 2182−2189.

(9) Chen, J. T.; Zhou, T. D.; Sun, W. B. Multifunctional lanthanide-based single-molecule magnets exhibiting luminescence thermometry and photochromic and ferroelectric properties. *Dalton Trans.* **2023**, *52*, 4643−4657.

(10) Sun, Y. H.; Li, C. L.; Wang, W. F.; Wang, S. H.; Li, P. X.; Guo, G. C. A photochromic and scintillation Eu-MOF with visual X-ray detection in bright and dark environments. *Chem. Commun.* **2022**, *58*, 4056−4059.

(11) Schubert, U. Cluster-based inorganic−organic hybrid materials. *Chem. Soc. Rev.* **2011**, *40*, 575−582.

(12) Xu, J.; Wang, J.; Ye, J.; Jiao, J.; Liu, Z.; Zhao, C.; Li, B.; Fu, Y. Metal-Coordinated Supramolecular Self-Assemblies for Cancer Theranostics. *Adv. Sci.* **2021**, *8*, No. 2101101.

(13) Reus, C.; Stolar, M.; Vanderkley, J.; Nebauer, J.; Baumgartner, T. A Convenient N-Arylation Route for Electron-Deficient Pyridines: The Case of π-Extended Electrochromic Phosphaviologens. *J. Am. Chem. Soc.* **2015**, *137*, 11710−11717.

(14) Jia, J. H.; Blake, A. J.; Champness, N. R.; Hubberstey, P.; Wilson, C.; Schröder, M. Multi-Dimensional Transition-Metal Coordination Polymers of 4,4′-Bipyridine-N,N′-dioxide: 1D Chains and 2D Sheets. *Inorg. Chem.* **2008**, *47*, 8652−8664.

(15) Zhang, N. N.; Han, Y. F.; Sun, C.; Wang, M. S.; Guo, G. C. Enhanced Photoinduced Electron Transfer and Stability of Diradicals in Neutral Extended Pyridine N-Oxides. *J. Phys. Chem. C* **2019**, *123*, 24670−24675.

(16) Sarma, R.; Baruah, J. B. Aromatic N-oxides in construction of different carboxylate coordination polymers of zinc(II), cadmium(II) and mercury(II). *Solid State Sci.* **2011**, *13*, 1692−1700.

(17) He, Y.; Huang, Y. R.; Li, Y. L.; Li, H. H.; Chen, Z. R.; Jiang, R. Encapsulating Halometallates into 3-D Lanthanide-Viologen Frameworks: Controllable Emissions, Reversible Thermochromism, Photocurrent Responses, and Electrical Bistability Behaviors. *Inorg. Chem.* **2019**, *58*, 13862−13880.

(18) Zhang, N. N.; Sa, R. J.; Sun, S. S.; Li, M. D.; Wang, M. S.; Guo, G. C. Photoresponsive triazole-based donor−acceptor molecules: color change and heat/air-stable diradicals. *J. Mater. Chem. C* **2019**, *7*, 3100−3104.

(19) Gong, T.; Yang, X.; Sui, Q.; Qi, Y.; Xi, F. G.; Gao, E. Q. Magnetic and photochromic properties of a manganese(II) metal-zwitterionic coordination polymer. *Inorg. Chem.* **2016**, *55*, 96−103.

(20) Sun, C.; Xu, G.; Jiang, X. M.; Wang, G. E.; Guo, P. Y.; Wang, M. S.; Guo, G. C. Design strategy for improving optical and electrical properties and stability of lead-halide semiconductors. *J. Am. Chem. Soc.* **2018**, *140*, 2805−2811.

(21) Benaissa, H.; Adarsh, N. N.; Robeyns, K.; Zakrzewski, J. J.; Chorazy, S.; Hooper, J. G. M.; Sagan, F.; Mitoraj, M. P.; Wolff, M.; Radi, S.; Garcia, Y. Exploring "Triazole-Thiourea" Based Ligands for the Self-Assembly of Photoluminescent Hg(II) Coordination Compounds. *Cryst. Growth Des.* **2021**, *21*, 3562−3581.

(22) Ma, Y. J.; Hu, J. X.; Han, S. D.; Pan, J.; Li, J. H.; Wang, G. M. Photochromism and photomagnetism in crystalline hybrid materials actuated by nonphotochromic units. *Chem. Commun.* **2019**, *55*, 5631−5634.

(23) Cai, L. Z.; Guo, P. Y.; Wang, M. S.; Guo, G. C. Photoinduced Magnetic Phase Transition and Remarkable Enhancement of Magnetization for a Photochromic Single-Molecule Magnet. *J. Mater. Chem. C* **2021**, *9*, 2231−2235.

(24) Yan, Y.; Zhang, N. N.; Börner, M.; Kersting, B.; Krautscheid, H. Hydroxamate based transition metal−organic coordination polymers with semiconductive properties. *Dalton Trans.* **2022**, *51*, 12709−12716.